Turkish J. Eng. Env. Sci.
33 (2009) , 281 – 293.

doi:10.3906/muh-0912-6

3D thermal finite element analysis of single pass girth welded low carbon steel pipe-flange joints

Muhammad ABID[1], **Muhammad Jawad QARNI**[2]
[1] *Associate Professor, Faculty of Mechanical Engineering, Ghulam Ishaq Khan Institute of Engineering Sciences and Technology, Topi-PAKISTAN*
e-mail: abid@giki.edu.pk
[2] *Research Associate, Faculty of Mechanical Engineering, Ghulam Ishaq Khan Institute of Engineering Sciences and Technology, Topi-PAKISTAN*
e-mail: jawadqarni@yahoo.com

Received 12.12.2009

Abstract

This paper presents a detailed computational procedure for predicting the complete thermal history including transient temperature distribution during girth welding and subsequent post weld cooling of low carbon steel pipe flange joints. Using the FE code ABAQUS, 3-dimensional non-linear heat transfer analysis is carried out to simulate gas metal arc welding (GMAW) process. ANSI Class #300 flange is used with a 6 mm thick, 200 mm long and 100 mm nominal diameter pipe. Joint type is a single 'V-groove' butt joint with a 1.2 mm root opening. FORTRAN subroutine is utilized for the application of volumetric heat flux from the weld torch using Goldak's double ellipsoidal heat source model, which is based on Gaussian power density distribution. Temperature dependent thermal properties as well as phase change effects have also been accounted. Apart from comprehensive discussion on the thermal history, in-depth analysis of the axial temperature profile at four different sections on both sides of the weld joint is presented. The simulated results showed that the temperature distribution around the implemented heat source model is steady when the weld torch moves around the circumferential joint. The present simulation model can be used as a proper tool to investigate the effect of different GMAW process parameters.

Key Words: Finite element analysis (FEA), girth GMAW process, pipe-flange joints, thermal history, transient temperature distribution.

Introduction

Pipe-flange joints are used in a number of high temperature and high pressure applications, such as applications in nuclear and petrochemicals industries. Performance of a flange joint is characterized mainly based on its 'strength' and 'sealing capability'. Prevention of fluid leakage is the prime requirement of the flange joints. Flange is joined to pipe usually by an arc welding process. Due to the concentrated heat of welding the region near the fusion zone (FZ) undergoes severe thermal cycles. Residual stresses and distortion build up, which affect the structural integrity of the joint. These distortions can lead to the poor sealing performance of the joint.

It is important for the function of a structure that welding residual stress field should be known quantitatively, as it may influence the mechanical behavior of structures including their fracture, stress corrosion cracking, fatigue, and buckling characteristics (Maddox, 1982).

As the intense heat of welding is the cause of residual stresses and distortions in a structure, much of analytical and numerical work on welding has been devoted to the heat source modeling of the welding torch. The basic theory of heat flow, which was developed by Fourier, was applied to the moving heat sources by Rosenthal (1946) and Rykalin (1974) for calculating the thermal history of the welds. Rosenthal's point or line models assumed that the flux and temperature were infinite at the heat source; therefore, they had high error in predicting temperature within the vicinity of fusion zone (FZ) and heat affected zone (HAZ). Finite element method (FEM) was used by several researchers to analyze heat flow in welding, in order to overcome earlier limitations of the analytical models. Pavelic et al. (1969) first suggested that the heat source should be distributed, and they proposed a Gaussian distribution of flux deposited on the surface of the workpiece. They presented a circular surface heat source and a hemispherical volume source. However, Pavelic's disc model still lacked the proper heat distribution throughout the molten zone and was not capable to reflect the digging action of the arc. Subsequently, in Paley and Hibbert (1975) and Westby (1968), a constant power density distribution was used in the FZ with finite difference method (FDM), but there were no criteria for estimating the length of the molten pool. FDM was also proved to be incapable of handling the complex geometry of real weld pools. Goldak et al. (1984, 1986) proposed a 3D "double ellipsoid" configuration heat source model. Both shallow and deep penetration welds as well as unsymmetrical situations can be accommodated. In the present work this model was used for the application of volumetric heat source.

This paper reports a thermal simulation using the FE code ABAQUS (2008) of GMAW process for a circumferential butt-welded low carbon steel pipe-flange joint using the FE transient heat transfer analysis. A weld neck flange of ANSI Class #300 with 8 holes for bolting is analyzed. The model comprises of a 200 mm long, 6 mm thick, and 100 mm nominal diameter pipe. Joint type was single 'V-groove' butt joint with a 1.2 mm root gap (Figure 1).

Thickness, T	Root Gap, R	Groove Angle, A	Root Face, F
6 mm	1.2 mm	60°	1.5 mm

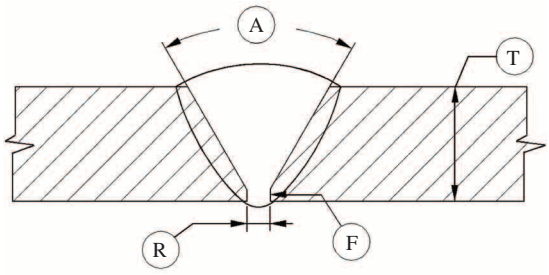

Figure 1. Geometry of the single-V groove weld joint design.

Material Modeling

Low carbon steel with a chemical composition of 0.18% C, 1.3% Mn, 0.3% Si, 0.3% Cr, and 0.4% Cu is used in present work. The complete range of temperature dependent thermal properties, such as specific heat capacity, heat conductivity, and density, were taken from the work of Karlsson and Josefson (1990).

During the analysis, melting behavior of the material was also taken into account. The heat in the weld pool is not only conducted but also convected due to the fluid flow. Therefore to model the fluid flow stirring effect, thermal conductivity was given an artificially higher value of 230W/m.K above the solidus temperature. This technique was suggested by Andersson (1978). This results in a uniform temperature within the weld pool and a relatively larger weld pool.

As suggested by Lindgren (2001), to model the phase change effects, latent heat of fusion is required. The latent heat of 272 KJ/Kg is defined over a temperature range of 1753 K to 1803 K i.e. the solidus and liquidus temperature, respectively. Temperature dependent thermal material properties in combination with latent heat effects are the cause of severe nonlinearity in the thermal solution.

Finite Element Model

The 3D FE model of pipe-flange joint (Figure 2a) contains a total of 17,456 nodes with associated 13,552 elements. Among these, 5952 elements are on the pipe side, whereas the remaining 7600 elements are on the flange side. Higher temperature and flux gradients are expected in and around the FZ and HAZ (Figure 2b); therefore, a relatively fine mesh is used within a distance of 10 mm on both sides of the weld centerline (WCL). Away from the HAZ, pipe and flange were divided into 3 regions of increasing element size as the distance from the WCL increases. Adaptive meshing was used throughout the study. For this purpose hexahedral transition elements are used on both sides of the weld groove. Care was taken in the mesh design so as to avoid the shape test warnings.

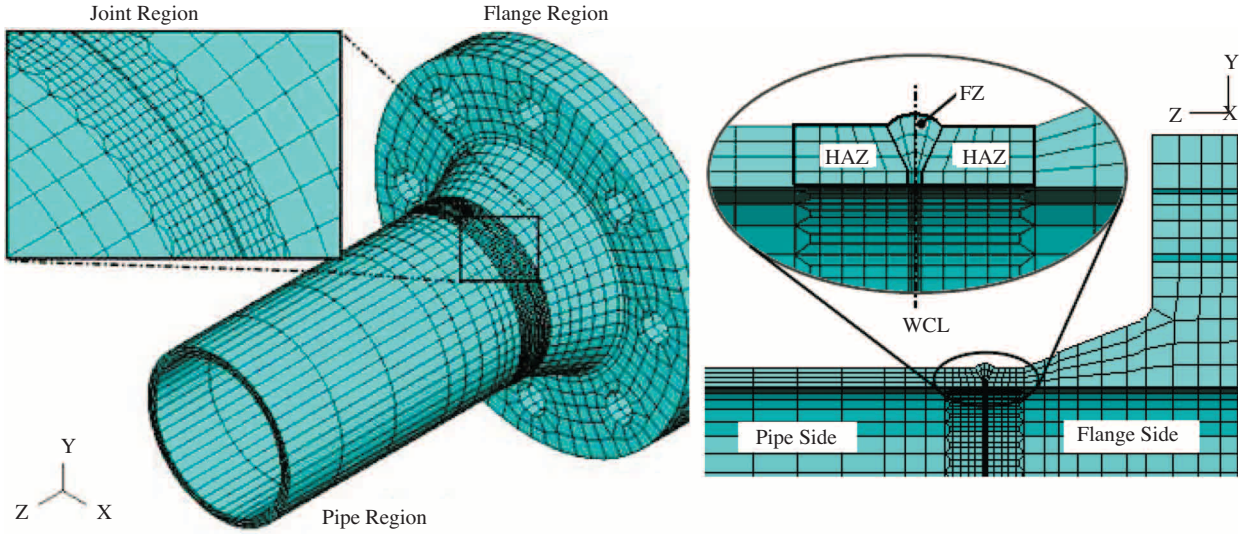

Figure 2. (a) Isometric view; (b) Sectioned view of the 3D finite element model of pipe-flange joint.

Being the area of a major concern, only the description of the element size in the FZ and HAZ is presented. In the axial direction, a distance of 10 mm on each side of the WCL represents the FZ and HAZ. Within this distance, the width of the FZ is divided into 4 elements, which vary from 0.3 to 1.5 mm, and the HAZ has 5 elements on each size of the weld centerline, where the element size varies from 1.2 to 1.8 mm. Within this anticipated HAZ, the entire periphery is divided into 144 elements, which gives the average length close to

2.5 mm. In the radial direction, the thickness is divided into 4 elements, each 1.5 mm, 3 of which make up the V-groove for the filler material. In the present study, for heat transfer analysis, solid (continuum) element DC3D8 is used from the ABAQUS elemental library. This is a 3D 8-noded linear brick (hexahedral) element, with a temperature as a single degree of freedom at each node. Further detail of this element can be found in ABAQUS (2008).

Thermal Analysis

Governing equations for thermal analysis

In heat transfer theory, we are concerned with energy and ignore stress, strain, and displacement. The conservation of energy is therefore the fundamental principle in thermal analysis. The governing equation for transient heat transfer analysis, during the welding is given by Equation 1:

$$\rho c \frac{\partial T}{\partial t}(x, y, z, t) = \nabla \cdot \vec{q}(x, y, z, t) + Q(x, y, z, t) \tag{1}$$

where ρ is the density of the materials, c is the specific heat capacity, T is the current temperature, $\vec{q}$ is the heat flux vector, Q is the internal heat generation rate, x, y and z are the coordinates in the reference system, t is the time, and σ is the spatial gradient operator.

Boundary conditions

To consider heat losses, both the thermal radiation and convection from the outer surface are assumed. Radiation losses are dominant for higher temperatures in and around the weld zone, where it becomes the primary mechanism of heat dissipation. Away from the weld zone at lower temperatures, convection plays a vital role in heat losses. Therefore, a combined heat transfer co-efficient is used, which is calculated from Equation 2 and is taken from Abid et al. (2005).

$$\widetilde{h} = \frac{\varepsilon_{em}\sigma_{bol}((T+273)^4 - (T_{amb}+273)^4)}{(T - T_{amb})} + h_{con} \tag{2}$$

where $\widetilde{h}$ is the combined heat transfer coefficient, $\varepsilon_{em}$is the emissivity, σ_{bol} is the Stefan Boltzmann constant, $T_{amb}$is the ambient temperature, and h_{con} is the convective heat transfer coefficient.

Heat source modeling

In the present study the so called "double ellipsoidal heat source model" (Figure 3) presented by Goldak et al. (1984, 1986) was used. This model, based on a Gaussian distribution of power density (W/m^3), has the capability of analyzing the thermal history of shallow and deep penetration welds (Goldak and Akhlaghi, 2005). Because of the inherent volumetric nature of this model, it effectively models the arc digging and stirring action and capable of transporting heat well below the surface of the weld pool. This model combines 2 ellipsoidal sources to simulate the actual experimental experience i.e. the temperature gradient in front of the source is steeper, compared to a gentler less steep gradient in the rear of the heat source.

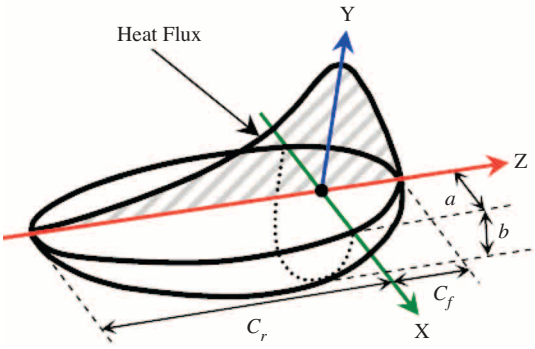

Figure 3. Double ellipsoid heat source configuration.

The power density distribution for this model, when expressed in moving Cartesian coordinate system (x, y and z), is depicted in Equations 3 and 4.

Distribution inside the front quadrant:

$$q_f(x,y,z,t) = \frac{6\sqrt{3}f_f Q}{abc_f\pi\sqrt{\pi}} exp\left\{-3\left(\frac{x^2}{a^2}+\frac{y^2}{b^2}+\frac{(z+\nu t)^2}{c_f^2}\right)\right\} \tag{3}$$

Similarly, for the rear quadrant:

$$q_r(x,y,z,t) = \frac{6\sqrt{3}f_r Q}{abc_r\pi\sqrt{\pi}} exp\left\{-3\left(\frac{x^2}{a^2}+\frac{y^2}{b^2}+\frac{(z+\nu t)^2}{c_r^2}\right)\right\} \tag{4}$$

where x, y,and z are the local spatial coordinates. $Q = \eta V I$ is the input power of the welding heat source. It is the product of the arc voltage (V), welding current (I), and process efficiency (η). ν is the welding speed and t is the current time. f_f and f_r are the heat fraction parameters in the front quadrant and rear quadrants, respectively, and where $f_f + f_r = 2.0$, the recommended values for these heat input fractions by Goldak et al. (1984) are $f_f = 0.6$ and $f_r = 1.4$. The equation that was originally described for plate welding is modified in order to make it appropriate for circumferential girth welding (Siddique, 2005).

The application of volumetric heat flux is achieved by implementing a user subroutine DFLUX, developed by the author in FORTRAN language. DFLUX subroutine provides user with an interface to define non-uniform distributed flux as function of time, position, temperature etc. during heat transfer analysis.

Numerical values for different parameters in double ellipsoidal power density distribution equation are taken from the work of Abid et al. (2005) and are given below in Tables 1 and 2.

Table 1. Numerical values for heat source parameters.

Parameter	Value	
Length of front ellipsoidal	a_f	12.9 mm
Length of rear ellipsoidal	a_r	10.3 mm
Depth of the heat source	b	6 mm
Width of the heat source	c	5 mm
Heat fraction (front)	f_f	1.4
Heat fraction (rear)	f_r	0.6

Table 2. Welding parameters.

Parameter	Value	
Welding Voltage	V	22 volts
Welding Current	I	225 amp
Weld Efficiency	η	85%

Procedure for analysis

The heat source moving at a speed of 6.25 mm/s around a diameter of 114.3 mm takes 58.7 s to complete a single revolution around the circumference. After the circumferential welding is completed, the joint is allowed to cool down. It takes about 50 min to return to the ambient temperature of approximately 300 K. During analysis 'Full Newton-Raphson' scheme is utilized. In this scheme, the complete Jacobian matrix is formed and solved at each iteration and is therefore expensive per iteration. However, this technique shows more flexibility to incorporate non-linear, i.e. temperature dependent, material properties. This scheme also exhibits faster convergence rates compared to other available methods, such as modified Newton or quasi-Newton methods. In order to improve the convergence, solution control option 'line search' was activated. In highly nonlinear problems (like the one presented in this work), the Newton algorithms may sometimes diverge during equilibrium iteration. The line search algorithm detects these situations automatically and applies a scale factor to the computed solution correction, which helps to prevent divergence.

Results and Discussion

Transient temperature distribution

Figure 4 shows the transient temperature distribution after 15 s of arc initiation. Figure 5a-f shows the temperature contours for 6 different time steps during and after the welding process. Here Figure 5a-c shows the

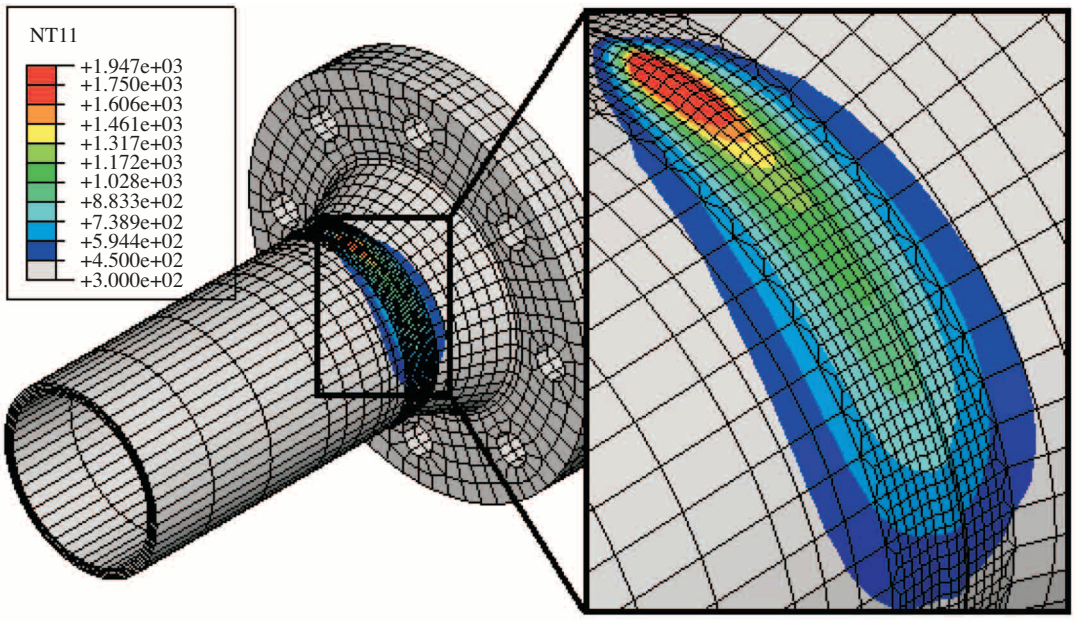

Figure 4. Transient temperature distribution (in Kelvins) after 15 s of arc initiation.

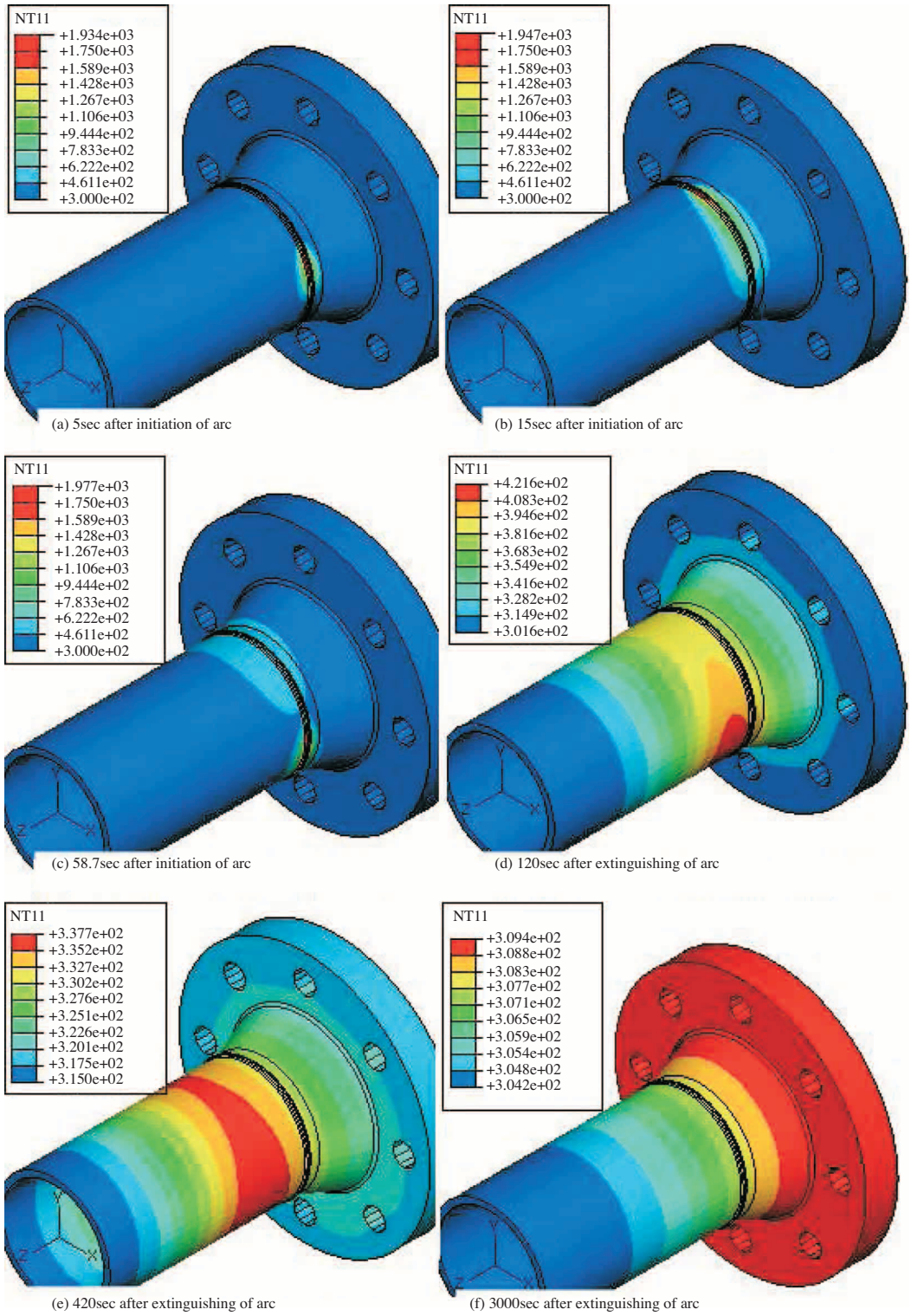

Figure 5. Temperature distribution (in Kelvin) at 6 different time steps.

temperature contours during the welding process. Figure 5d-f shows temperature contours after welding has been completed, and the joint is allowed to cool. As predicted the maximum temperatures are observed at the heat source location (i.e. close proximity to the weld line). Steep temperature gradients are observed ahead of the heat source, showing the least significance of heat flow ahead of the welding torch. The gradients behind the heat source show the cooling phenomenon after the peak temperature achieved, as the heat source moves ahead from a certain point. Figure 5f shows the final temperature distribution when the joint has been given enough time to cool to almost the ambient temperature of the surroundings. Notice that comparably somewhat higher temperatures are found on the flange side. Higher thermal inertia (i.e. ability of a body to store internal energy) of the flange is believed to be the cause.

Temperature history

Figure 6 shows welding temperature history on the time-temperature axes of a point at the WCL on the outer surface. The plots represent what happens at that point on the weldment as a function of time; from just before the heat source acting on the point to just after the heat source is removed from the point. Important aspects to be considered are as follows:

1. The temperature starts out at the ambient temperature of the environment i.e. 300 K, prior to the arrival of a moving heat source.
2. The temperature rises very rapidly once the heat source reaches the point.
3. The temperature reaches a maximum peak of 1947 K. This is determined by the balance between the energy being inputted and all losses.
4. The temperature remains at that maximum only as long as the source remains on that point, which for this case is only an instant, as the heat source is moving with some velocity.
5. The temperature cools back to the ambient level at a rate dependent on the thermal mass and thermal-physical properties of the material.

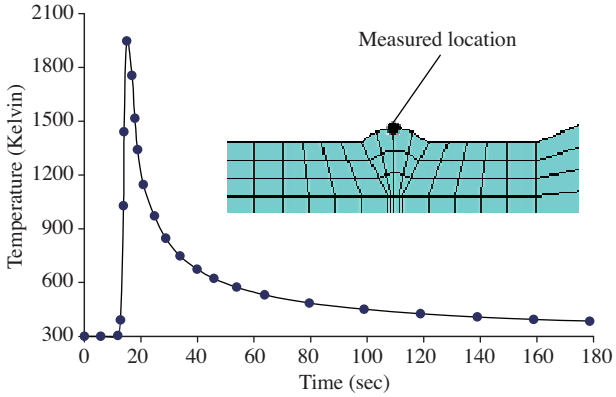

Figure 6. Temperature history of a point at the weld center line.

In Figure 6 notice that the peak temperature is well above the liquidus temperature of low carbon steel. This is important to ensure that melting is complete and that sufficient fluidity is achieved to allow material to flow into the weld groove properly. After the heat source has passed that point, the cooling of the newly formed

joint is quite rapid. This is evident from the temperature values of the thermal analysis, at the 15^{th} second the temperature is 1947 K and at the 25^{th} second (i.e. 10 seconds later) this temperature has dropped to 964 K. This shows that the temperature is decreasing at a rate of several hundred degrees per second. The reason for this rapid temperature drop is that radiation is the dominant heat loss mechanism at higher temperatures and later on convection comes into action at somewhat lower temperatures. It is this temperature-time history within this heat-affected region that determines the effect on the base material surrounding the region of fusion (i.e., the HAZ).

It is also important to ensure that the heat input by the weld torch is consistent throughout the duration of welding, and that it should not vary too much. Different points along axial direction were selected as shown in Figure 7, both at pipe side and flange side. Four different cross-sections i.e. at 45°, 135°, 225° and 315° (Figure 8), were selected. The transient temperature histories along these selected cross-sections are presented in Figure 9a-d. As can be seen in the figures, the temperature history and peak temperatures obtained are almost identical and therefore it can be concluded that the temperature history is not sensitive to the variations in the angle defined with respect to the weld start position.

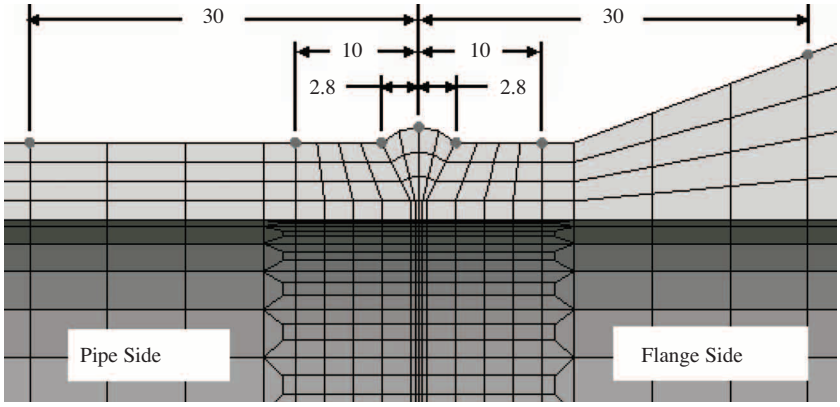

Figure 7. Illustration of axial location where the temperature values were recorded.

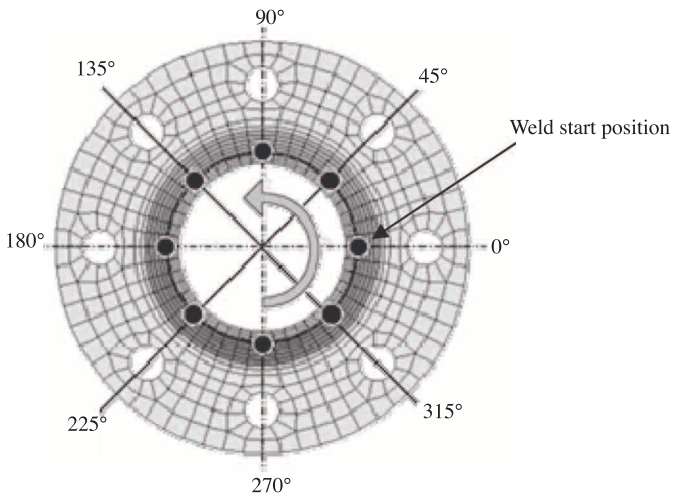

Figure 8. Angular locations from the weld start position.

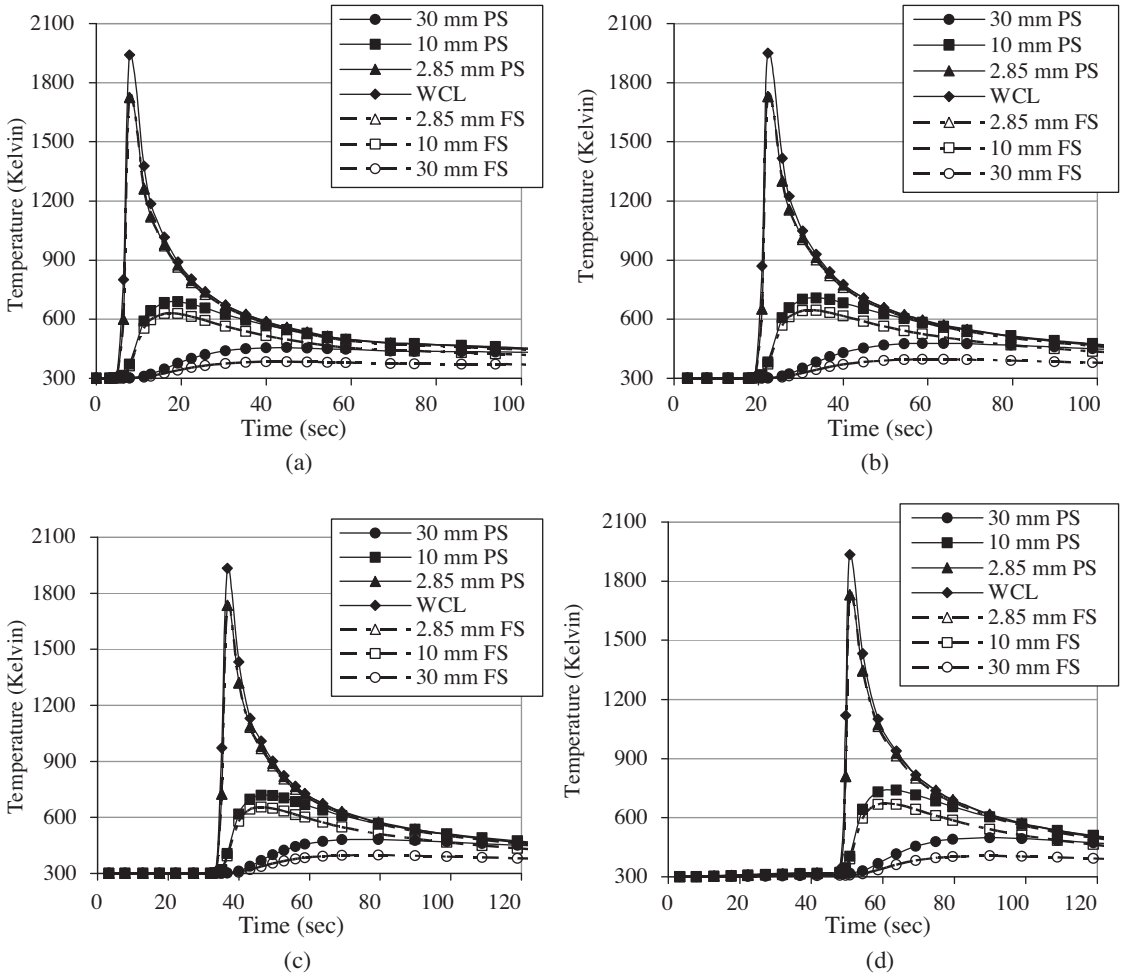

Figure 9. Temperature histories at various distances from WCL at (a) 45° (b) 135° (c) 225° and (d) 315° from the weld start position.

Axial temperature profiles

Figure 10 shows the 2D sectional view of the pipe flange joint on a millimeter scale; this is presented for better visualization of the axial dimensions of the joint.

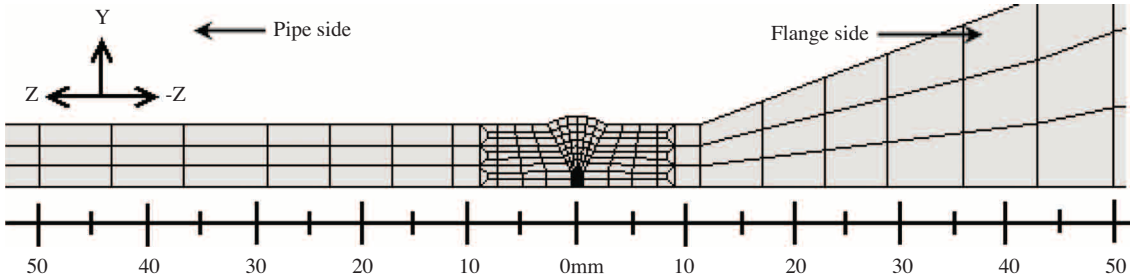

Figure 10. Partial view of the axial cross-section along mm scale.

Axial temperature distribution in the vicinity of FZ is presented in Figure 11. Notice that the temperature falls gradually within the width of the weld groove, which is 2.85mm per side of the WCL. This is because the

heat source parameters (a, b, & c) are defined so as to cover the width and depth of the weld groove. However, temperature distribution away from the weld groove suffers a rapid decline.

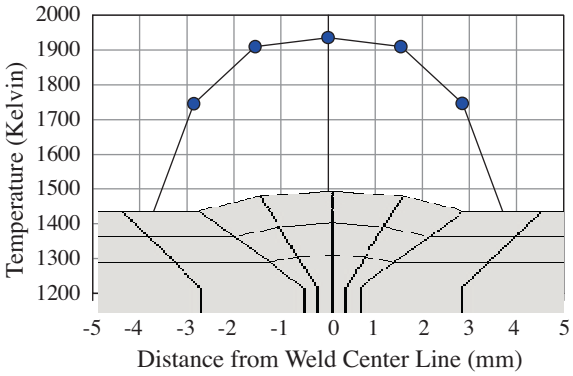

Figure 11. Temperature profile at the weld groove width along 90° from weld start position.

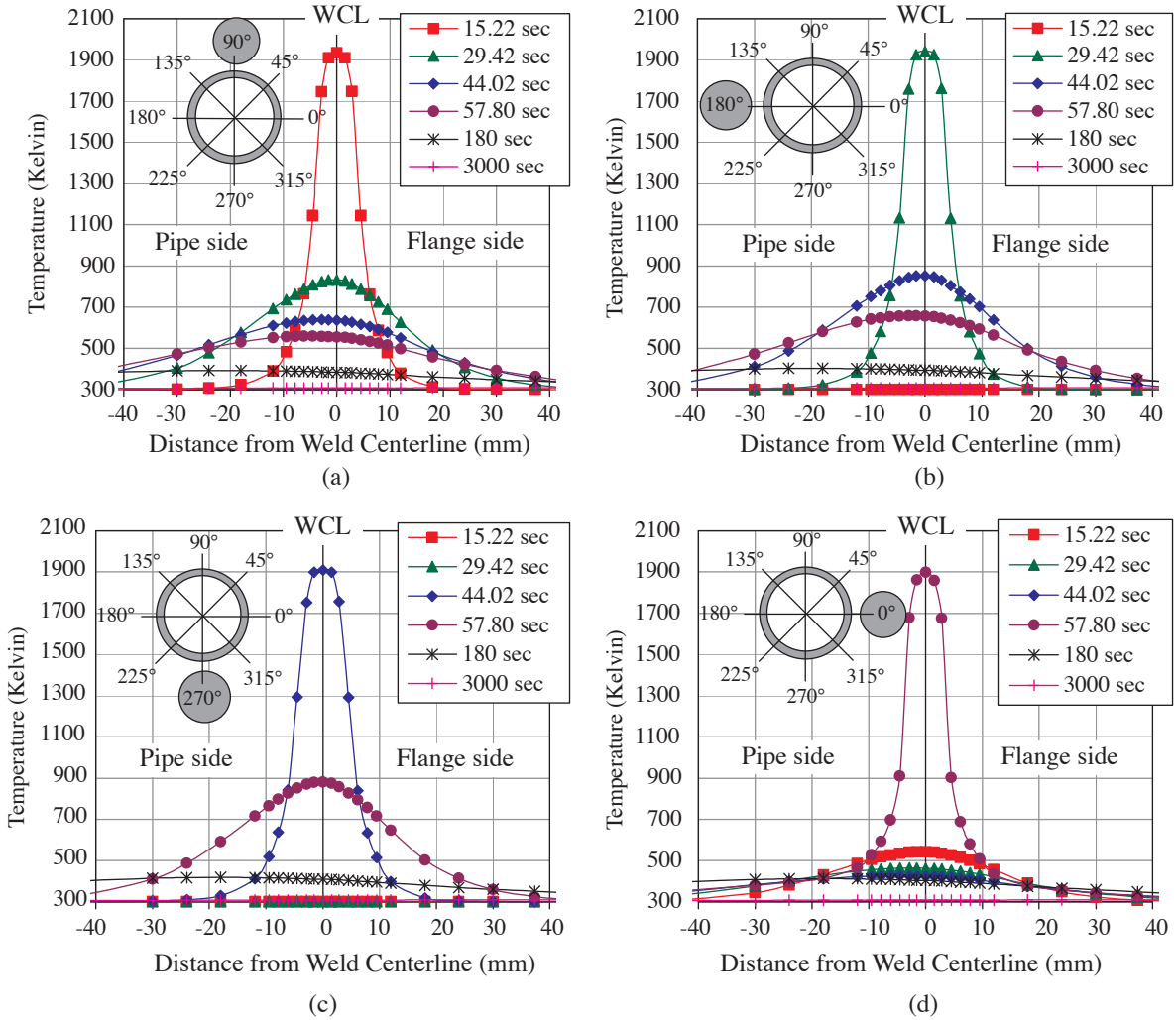

Figure 12. Axial temperature profile at a cross-section of (a) 90°, (b) 180°, (c) 270°, and (d) 360° at various time steps.

Figure 12a-d shows the axial temperature distributions profiles for 4 different cross-sections (90°, 180°, 270°, and 360°/0°) at different time steps taken at either side of the weld centerline (WCL). In Figure 12a, the section is located at an angle of 90° from the weld start position. The heat source traveling with welding speed of 6.25 mm/s around the circumference of 359.1 mm reaches the section after 15.22 s. Therefore, the maximum temperature as anticipated is observed at the heat source position. The temperature falls down slowly as the heat source crosses the section. Also notice that the profile is not symmetric along the WCL; this is mainly due to the geometrical difference between the pipe and the flange. As a general observation temperature gradient at the pipe side is higher than at the flange side, low thickness of the pipe as compared to the flange is considered to be the cause, therefore the pipe gets heated up more quickly.

Conclusion

Following conclusions are drawn from the study:

1. The temperature distribution in the developed 3D FE models of single pass welding was reasonably steady around the heat source during the welding process of the pipe flange joint of low carbon and stainless steel.
2. The axial temperature distribution on both sides of the weld centerline beyond the anticipated HAZ was not symmetrical, because of the unsymmetrical geometry of pipe-flange joint. Due to this fact, the assumption of FE model symmetry at the weld centerline is not applicable for the pipe-flange joint.
3. Beyond the anticipated HAZ, temperature gradients at the pipe side reach higher values as compared to the values on the flange side. As compared to the wall thickness of the flange, pipe has a low thickness and therefore gets heated up more quickly. The pipe was found to be 50 to 80 K higher in temperature.
4. Despite the fact that pipe side reaches higher temperature values, the pipe side dissipates heat more quickly as compared to the flange side. Flange side possessing a greater thermal inertia was found to take longer time to cool as compared to pipe, at least for the flange class used in the present study.
5. Using this FE model, a parametric study can be performed for the process variables, such as the welding current, voltage, and efficiency, preheating temperature of the work piece, welding velocity, and the path sequence of the welding procedure. Extension of this work is in progress to couple with a mechanical model to simulate the thermal stress developed during the process and dimensional accuracy of the welded pipes.

References

"ABAQUS Version 6.8", Analysis User's Manual, 2008.

Abid, M., Siddique, M. and Mufti, R. A., "Prediction of Welding Distortions and Residual Stress in Pipe-Flange Joint Using Finite Element Technique", Model. Simul. Mater. Sci. Eng., 13, 455-470, 2005.

Andersson, B. A. B., "Thermal Stresses in a Submerged-Arc Welded Joint Considering Phase Transformations", J Eng. & Tech. Trans. ASME, 100, 356-362, 1978.

Goldak, J., Chakravarti, A. and Bibby, M., "A New Finite Element Model for Heat Sources", Metall. Trans. B, 15B, 299-305, 1984.

Goldak, J., Bibby, M., Moore, J., House, R. and Patel, B., "Computer Modeling of Heat Flow in Welds", Metallurgical Transactions B, 17, 587-600, 1986.

Goldak, J. and Akhlaghi, M., "Computational Welding Mechanics", e-ISBN. 0-387-23288-5, Springer, 2005.

Karlsson R. I. and Josefson, B. L.: "Three Dimensional Finite Element Analysis of Temperature and Stresses in Single-Pass Butt-Welded Pipe", ASME J. PVT, 112, 76-84, 1990.

Lindgren, L. E., "Finite Element Modeling and Simulation. Part 2: Improved Material Modeling", Journal of Thermal Stresses, 24, 195-231, 2001.

Maddox, S. J., "Influence of Tensile Residual Stresses on the Fatigue Behavior of Welded Joints in Steel", American Society for Testing and Materials, STP 776, 63-96, 1982.

Paley, Z. and Hibbert P.D., "Computation of Temperatures in Actual Weld Designs", Welding Journal Research Supplement, 54, 385s-392s, 1975.

Pavelic, V., Tanbakuchi, R., Uyehara, O. A. and Myers., "Experimental and Computed Temperature Histories in Gas Tungsten Arc Welding of Thin Plate", Welding Journal Research Supplement, 48, 259s-305s, 1969.

Rosenthal, D., "The Theory of Moving Sources of Heat and its Application to Metal Treatments", Trans ASME, 68, 849-865, 1946.

Rykalin, R. R., "Energy Sources for Welding", Welding in the World, 12, 9/10, 227-248, 1974.

Siddique, M., "Experimental and Finite Element Investigation of Residual Stresses and Distortion in Welded Pipe and flange Joints", Ph.D. Thesis, Ghulam Ishaq Khan Institute, 2005.

Westby, O., "Temperature Distribution in the Workpiece by Welding, Department of Metallurgy and Metals Working, The Technical University, Trondheim Norway", 1968.